Anisotropy of the electric properties of alloys of terbium, gadolinium, and yttrium

S. A. Nikitin

Moscow State University
(Submitted 5 December 1980)
Zh. Eksp. Teor. Fiz. **80**, 2409–2414 (June 1981)

The concentration and temperature dependences of the anisotropy of the electric resistivity of single crystals of the alloys Tb–Gd, Tb–Y, and Dy–Y is investigated. It is shown that the strong anisotropy of the resistivity of the ferromagnetic Tb–Gd alloys is due mainly to the anisotropy of the magnetic contribution ρ_M to the resistivity; this anisotropy increases sharply with increasing Tb content in Gd. This anisotropy can be attributed to scattering due to Coulomb interaction between the conduction electrons and to the anisotropy of the $4f$-electron shell of the Tb ions with orbital angular momentum $L \neq 0$. The increase of the anisotropy of ρ_M in the antiferromagnetic Tb–Y and Dy–Y alloys in the paramagnetic region observed following magnetic dilution of the Tb and Dy by yttrium is attributed to conduction-electron s–f exchange scattering, the anisotropy of which increases with increasing stability of antiferromagnetic helicoidal structure.

PACS numbers: 72.15.Eb

The electric properties of rare-earth metals (REM) have considerable anisotropy. An analysis of the experimental data has led to the conclusion that the cause of this anisotropy is that both the phonon and magnetic contributions ρ_{ph} and ρ_M to the resistivity are anisotropic.[1–5] The anisotropy of ρ_{ph} is usually ascribed to the anisotropy of the carrier effective mass, which is the result of the complicated topology of the Fermi surfaces of REM.[6] To explain the anisotropy of ρ_M, a number of mechanisms were theoretically investigated.[7–10] The experimental results for REM, however, do not indicate unambiguously which of these mechanisms predominates.

To ascertain the influence of various factors on the anisotropy of the electric properties of REM and their alloys, we have investigated experimentally the anisotropy of the electric resistivity of binary alloys of terbium, dysprosium, gadolinium, and yttrium, in which one can vary the density of REM ions having orbital angular momentum, as well as the height of the energy barrier between the ferromagnetic and antiferromagnetic helical structures. This allows the mechanisms responsible for the anisotropy of the magnetic scattering of the carriers to be separated.

The technology of the growth of single crystals of the alloys and of monitoring their quality, as well as the technique of the resistivity measurements, were reported earlier.[3–5] We determined the anisotropies of the phonon and magnetic contributions ρ_{ph} and ρ_M by measuring the concentration and temperature dependences of the resistivity along the principal crystallographic directions a, b, and c, followed by separating these contributions by the previously described method.[3–5]

Figures 1–3 show, for the alloys Tb_xGd_{1-x}, Dy_xY_{1-x}, and Tb_xY_{1-x}, the concentration dependences of the anisotropy $\vartheta_\perp = 2(\rho_M^a - \rho_M^b)/(\rho_M^a + \rho_M^b)$ of the magnetic part of the resistivity in the paramagnetic region for the basal plane, and the anisotropy $\vartheta_\parallel = 2(\rho_M^a - \rho_M^c)/(\rho_M^a + \rho_M^c)$ for the plane containing the a and c axes, where ρ_M^i is the magnetic contribution along the i-th axis. The figures show

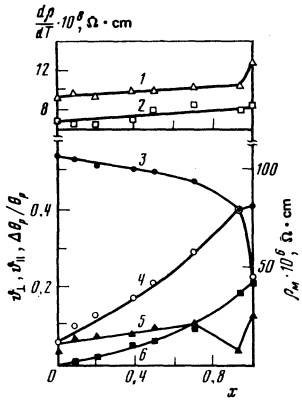

FIG. 1. Concentration dependence of the electric properties of Tb_xGd_{x-1} alloys in the paramagnetic region: 1) temperature coefficient of resistivity $d\rho^a/dT$ along the a axis; 2) $d\rho^c/dT$ along the c axis; 3) magnetic contribution ρ_M^a to the resistivity; 4) anisotropy $\vartheta_\parallel$ of magnetic contribution to the resistivity in the ac plane; 5) anisotropy $\vartheta_\perp$ of the magnetic contribution in the ab plane; c) anistropy $d^{\mathrm{Tc}}_{\rho}/^{\mathrm{Tc}}_{\rho}$ of the paramagnetic Curie point.

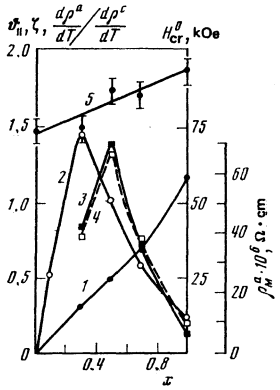

FIG. 2. Concentration dependence of the electric properties and of the critical field H_{cr}^0 in Dy_xY_{1-x} alloys: 1) magnetic contribution ρ_M^a to the resistivity along the a axis at $T > \Theta_2$; 2) $H_{cr}{}^0$; 3) anisotropy $\vartheta_\parallel$ of the magnetic contribution to the resistivity in the ac plane (points ■); 4) relative increase ζ of the magnetic contribution ρ_M^c at the point Θ_2 (points □); 5) anisotropy of temperature coefficients of the resistivity, $d\rho^a/dT/d\rho^c/dT$ in the paramagnetic region at $T > \Theta_2$.

 0038-5646/81/061260-04$02.40

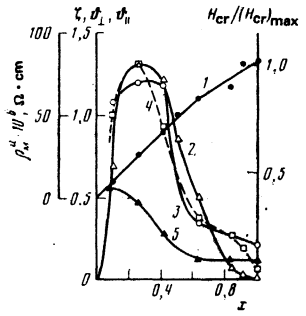

FIG. 3. Concentration dependence of the electric properties and of the critical field H_{cr}^0 in Tb_xY_{1-x} alloys: 1) magnetic contribution ρ_M^a to the resistivity along the a axis in the paramagnetic reation near $T > \Theta_2$; 2) relative value of H_{cr}^0; 3) anisotropy $\vartheta_\parallel$ of magnetic contribution to the resistivity in the ac plane (points ○); 4) relative increase of the contribution ρ_M^c at the point Θ_2 (points □); 5) anisotropy $\vartheta_\perp$ of the magnetic contribution to the resistivity in the ab plane.

also the concentration dependences of the magnetic contribution to the resistivity in the basal plane along the a axis, due mainly to scattering of the conduction electrons by magnetic inhomogeneities on account of s–f exchange interaction.[3-5]

The anisotropy of ρ_M in gadolinium is weak ($\vartheta_\perp \sim 0.03$ and $\vartheta_\parallel \sim 0.05$). Introduction of terbium ions into gadolinium causes a strong increase of the anisotropy of the magnetic contribution: $\vartheta_\perp$ is increased by three times (Fig. 1, curve 5) and $\vartheta_\parallel$ by 6 times when 70% Tb is introduced into gadolinium (Fig. 1, curve 4). It is important that in this case, as seen from Fig. 1 (curves 1 and 2) the anisotropy of the phonon contribution ρ_{ph} does not change: $(d\rho_{ph}^a/dT)\,(d\rho_{ph}^c/dT)^{-1} \approx 1.3$. This means that the effective-mass anisotropy $m''/m\,(d\rho_{ph}^a/dT)(d\rho_{ph}^c/dT)^{-1}$ in Tb_xGd_{1-x} alloys remains approximately constant in the concentration interval $0 < x < 0.9$.

It was shown earlier that Tb_xGd_{1-x} alloys[4] with $x < 0.94$ are ferromagnets in the magnetically ordered state. The decrease of the magnetic contribution ρ_M^a in the basal plane with increasing terbium concentration, observed in Fig. 1 (curve 3), is due to the decreased conduction-electron scattering on account of s–f exchange. Thus, the increase of the anisotropy of ρ_M with increasing terbium concentration in these alloys cannot be attributed to increases of the anisotropy of the effective mass and of the s–f exchange interaction.

The most probable mechanism responsible for the strong growth of the anisotropy of the resistivity with increasing terbium content in terbium-gadolinium alloys is the scattering of the carriers by the inhomogeneities of the quadrupole moments of 4f subshells, which, according to the theory of Irkhin *et al.*,[7,8] leads to anisotropy of the relaxation time in accordance with the following formula for the anisotropy of the magnetic part of the resistivity of REM in the paramagnetic region:

$$\frac{\Delta\rho_M^{ij}}{\rho_M^{ij}} = \frac{\Delta m^{ij}}{\bar{m}_{ij}} + \beta_J \frac{\Delta\varphi_{ij}}{1+\beta_J\bar{\varphi}_{ij}}, \qquad (1)$$

where $i, j = a, b, c$; the first term takes into account the carrier effective mass anisotropy, and the second the relaxation-time anisotropy on account of quadrupole scattering. The quantities $\bar{\varphi}_{ij}$ and $\Delta\varphi_{ij}$ are linearly connected with the coefficients of the expansion of the crystal potential in the lattice reciprocal vectors. β_J is given by

$$\beta_J = \left(\frac{9}{5\sqrt{2}}\right)^2 \frac{\alpha^2 J(J+1)}{(g_J-1)^2}\left(\frac{F}{I}\right)^2, \qquad (2)$$

where S, L, and J are the REM-ion quantum numbers, $\alpha = \alpha(S, L, J)$ is the Stevens factor,[7] F is the integral of the Coulomb interaction of the conduction electrons with the localized 4f electrons, and I is the s–f exchange integral.

It follows from (1) and (2) that the anisotropy of the magnetic part of the resistivity depends on the anisotropy of the effective mass, on the atomic constants of the REM ions, and on the square of the ratio of the quadrupole Coulomb scattering to the isotropic s–f exchange scattering.

The Tb^{3+} ions located at the crystal lattice sites of these alloys have an anisotropic electron 4f subshell with orbital momentum $L = 3$, while the Gd^{3+} ions have a spherical electron 4f subshell with $L = 0$. Therefore an increase of the terbium-ion concentration in Tb_xGd_{1-x} alloys should lead to an increase of the resultant quadrupole scattering and to an increase of the resistivity anisotropy $\vartheta_\parallel$ and $\vartheta_\perp$ in the paramagnetic region, as is observed in experiment (Fig. 1, curves 4 and 5). This conclusion is confirmed also by the fact that the anisotropy $\Delta\Theta p/\Theta p$ of the paramagnetic Curie point (curve 6 of Fig. 1), which is proportional to the ratio of the energy of interaction of the orbital momenta with the crystal field to the exchange energy, also increases with increasing terbium content in Tb_xGd_{1-x} alloys.

The singularities in the concentration dependences of ρ_M, $\vartheta_\parallel$, and $\vartheta_\perp$ at $x > 0.94$ (see Fig. 2, curves 4 and 5) can be attributed to a change of the effective-mass anisotropy

$$\frac{m_\parallel}{m_\perp} \approx \frac{d\rho_{ph}^a}{dT} \Big/ \frac{d\rho_{ph}^c}{dT},$$

which increases sharply at $x > 0.94$, as follows from curves 1 and 2 of Fig. 1. This raises the question whether the resistivity-anisotropy mechanisms considered by us for the Tb_xGd_{1-x} alloys are sufficient to explain the anisotropy of the magnetic contribution in the alloys Tb_xY_{1-x} and Dy_xY_{1-x}, which undergo a helicoidal antiferromagnetism–ferromagnetism transition atthe termperature Θ_2.

Where terbium and dysprosium are magnetically diluted with yttrium, the number of ions participating in the s–f exchange interaction decreases. As a result the scattering of the conduction electrons in the paramagnetic region by magnetic inhomogeneities, due to s–f exchange, is decreased, a fact manifest in the almost linear decrease of the corresponding magnetic contribution to the resistivity in the basal plane with increasing yttrium content (curves 1 in Figs. 2 and 3). When heavy REM are diluted with yttrium, one should expect also a decrease of the resultant quadrupole scattering, aince the number of ions with $L \neq 0$ decreases.

The experimental data, nonetheless, point to a strong increase of the anisotropy of the magnetic contribution and of the anisotropy of the total resistivity, determined in the paramagnetic region, when Dy and Tb are diluted with yttrium; the values of $\vartheta_\parallel$ (curves 3 on Figs. 2 and 3) and $\vartheta_\perp$ (Fig. 3, curve 5) increase by several times in the diluted alloys relative to Tb and Dy. The resistivity in the basal plane in certain dilute alloys is more than double the resistivity along the c axis. For example, the ideal resistivity at $T = 125$ K along the a and c axes in $Dy_{0.49}Y_{0.51}$ are $\rho^a = 72\ \mu\Omega \cdot$ cm and $\rho^c = 41\ \mu\Omega \cdot$ cm, while in $Tb_{0.26}Y_{0.74}$ the values are $\rho^a = 55\ \mu\Omega \cdot$ cm and $\rho^c = 18\ \mu\Omega \cdot$ cm. The resistivities of Tb and Dy are not so strongly anisotropic. After reaching a certain maximum following magnetic dilution (at $x \approx 0.5$ in alloys with Dy and at $x \approx 0.3$ in alloys with Tb), the anisotropy $\vartheta_\parallel$ decreases.

A similar behavior of the concentration-dependence curves is observed (curves 2 of Figs. 2 and 3) for the maximum critical magnetic field H_{cr} at which the antiferromagnetism–ferromagnetism transition takes place, and for the quantity

$$\zeta = (\Delta\rho_M)_{T=\Theta_2} / (\rho_M)_{T>\Theta_2},$$

which determines the increase of the magnetic contribution ρ_M near the temperature Θ_2 along the c axis (curves 4 on Fig. 2 and 3). It should be noted that ζ and $\vartheta_\parallel$ have close values in a number of alloys.

The anisotropy of ρ_{ph} in Dy_xY_{1-x} alloys with large yttrium concentration is smaller than that of Dy (curve 5 of Fig. 2). The resultant decrease of the anisotropy $\Delta m/m$ should lead, according to (1), to a decrease of $\vartheta_\parallel$, in contradiction to the observed effect. A similar conclusion can be drawn also from the experimental data for the Tb_xY_{1-x} alloys.

To explain the experimental results on the electric properties of heavy REM alloys with yttrium, it is necessary to invoke, in our opinion, besides the already indicated resistivity-anisotropy mechanisms, also the scattering of conduction electrons by magnetic inhomogeneities on account of the s–f exchange interaction, which can have an anisotropic character in alloys with helical magnetic structure even in the paramagnetic region.

According to neutron-diffraction data,[11] at temperatures above the point Θ_2 there exist in heavy REM, in the paramagnetic region, spin-system excitations characterized by a local helical magnetic structure with wave vector $q \neq 0$ and with a period close to the pitch of the helix at $T = \Theta_2$. On the other hand, as established theoretically by Vedyaev and Usmanov,[10] the scattering of conduction electrons by magnons with wave vector $q \neq 0$ as a result of s–f exchange has a strong anisotropy due to the anisotropic dispersion law of the magnons. It can be assumed that in this case, if the antiferromagnetic helical structure becomes more stable (high values of H_{cr}), then excitations of magnons with $q \neq 0$ at $T > \Theta_2$ are more probable, and this leads to a strong anisotropy of the conduction-electron scattering in the paramagnetic region.

The anisotropy of the magnetic part of the resistivity

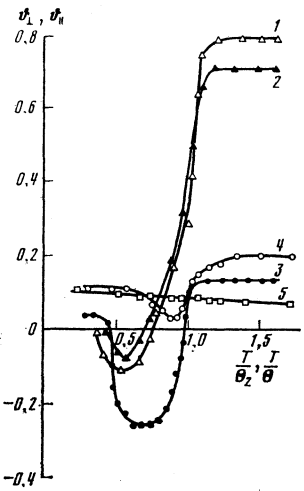

FIG. 4. Temperature dependence of the anisotropy of the magnetic contribution to the electric resistivity in dysprosium-yttrium and terbium-gadolinium alloys: 1) $\vartheta_\parallel(T/\Theta_2)$ in the alloy $Dy_{0.305}Y_{0.695}$; 2) $\vartheta_\parallel(T/\Theta_2)$ in the alloy $Dy_{0.69}Y_{0.31}$; 3) $\vartheta_\parallel(T/\Theta_2)$ in Dy; 4) $\vartheta_\parallel(T/\Theta)$ in the alloy $Tb_{0.5}Gd_{0.5}$; 5) $\vartheta_\perp(T/\Theta)$ in the alloy $Tb_{0.5}Gd_{0.5}$.

remains practically unchanged if $T > \Theta_2$, but cooling below Θ_2 causes a decrease of $\vartheta_\parallel$ (curves 1–4 of Fig. 4), whereas $\vartheta_\perp$ changes relatively little (curve 5 of Fig. 4). The decrease of $\vartheta_\parallel$ at $T < \Theta_2$ is due to the appearance of an energy gap in the conduction-electron spectrum[8,9] because of formation of superband boundaries perpendicular to the axis of the antiferromagnetic helicoidal structure. The effect of the gap is so appreciable that in Dy and its alloys the sign of $\vartheta_\parallel$ is reversed at $T < \Theta_2$, with a second change of sign of $\vartheta_\parallel$ in Dy at the ferromagnetism–antiferromagnetism transition point $\Theta_1 = 85$ K (curve 3 of Fig. 4).

The contribution made to the resistivity anisotropy δ by the gap is negative and exists only for $\vartheta_\parallel$ (Ref. 8):

$$\delta = \frac{\pi m \Delta}{(2mE_F)^{1/2} 2\hbar^2 l}, \qquad (3)$$

where l is the wave vector along the discontinuity line, and Δ is the size of the gap and is proportional to the magnetization m.

An alternative of this mechanism of anisotropy decrease at $T < \Theta_2$ is the increase of ρ_M^c due to critical fluctuations near the point Θ_2. In this case we can explain the agreement between $\vartheta_\parallel$ and ζ experimentally observed by us for dysprosium-yttrium alloys (curves 3 and 4 of Figs. 2 and 3). Final conclusions, however, call for further theoretical and experimental investigations.

In conclusion, the author thanks K. P. Belov for valuable remarks made in the discussion of the final results, V. P. Posyado for help with the work, and G. E. Chiprikov and O. D. Chistyakov for supplying the alloy single crystals.

[1]S. Levgold, in: Magnetic Properties of Rare Earth Metals, R. J. Elliott, ed., Plenum, 1971, pp. 335–380.
[2]N. V. Volkenshtei, V. P. Dyakina, and V. E. Startsev, Phys.

Stat. Sol. (b) 57, 9 (1973).
[3]K. P. Belov, S. A. Nikitin, V. P. Starkov, and G. E. Chuprikov, Zh. Eksp. Teor. Fiz. **71**, 2204 (1976) [Sov. Phys. JETP **44**, 1162 (1976)].
[4]S. A. Nikitin, N. A. Sheludko, V. P. Posado, and G. E. Chuprikov, *ibid.* **73**, 1002 (1977) [**46**, 530 (1977)].
[5]S. A. Nikitin, S. M. Nakvi, I. K. Solomkin, and O. D. Chityakov, Fiz. Tverd. Tela (Leningrad) **19**, 2301 (1977) [Sov. Phys. Solid State **19**, 1347 (1977)].
[6]A. Freeman, in: op. cit.[1], pp 258–320.
[7]Yu. P. Irkhin, L. T. Raevskaya, and Sh. Sh. Abel'skiĭ, Fiz. Tverd. Tela (Leningrad) **19**, 3363 (1977) [Sov. Phys. Solid State **19**, 1964 (1977)].
[8]L. T. Raevskaya, Sh. Sh. Abel'skiĭ, and Yu. P. Irkhin, *ibid.* **20**, 3341 (1978) [**20**, 1928 (1978)].
[9]R. Elliott and F. Wedgewood, Proc. Phys. Soc. **81**, 846 (1963).
[10]A. V. Vedyaev and M. Kh. Usmanov, Izv. AN UzSSR No. 3, 37 (1980).
[11]A. G. Mandzhavidze and G. A. Kharadze, Pis'ma Zh. Eksp. Teor. Fiz. **10**, 68 (1969) [JETP Lett. **10**, 44 (1969)].

Translated by J. G. Adashko